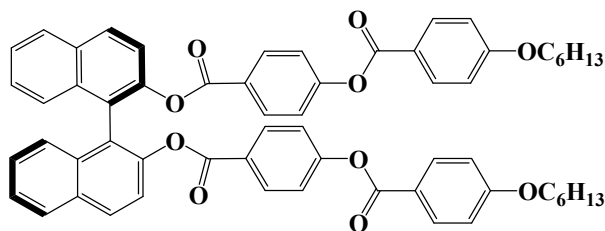


Supporting Information

Phototuning Structural Color and optical switching cholesteric textures in Azobenzene-Doped Cholesteric Liquid Crystals

Hongbo Lu ^{a, b*}, Ying Cao ^{a, b}, Hao Bai ^{a, c}, Mingyan Ren ^{a, c}, Longzhen Qiu ^{a, c}, Jun Zhu ^{a, b},
Miao Xu ^a

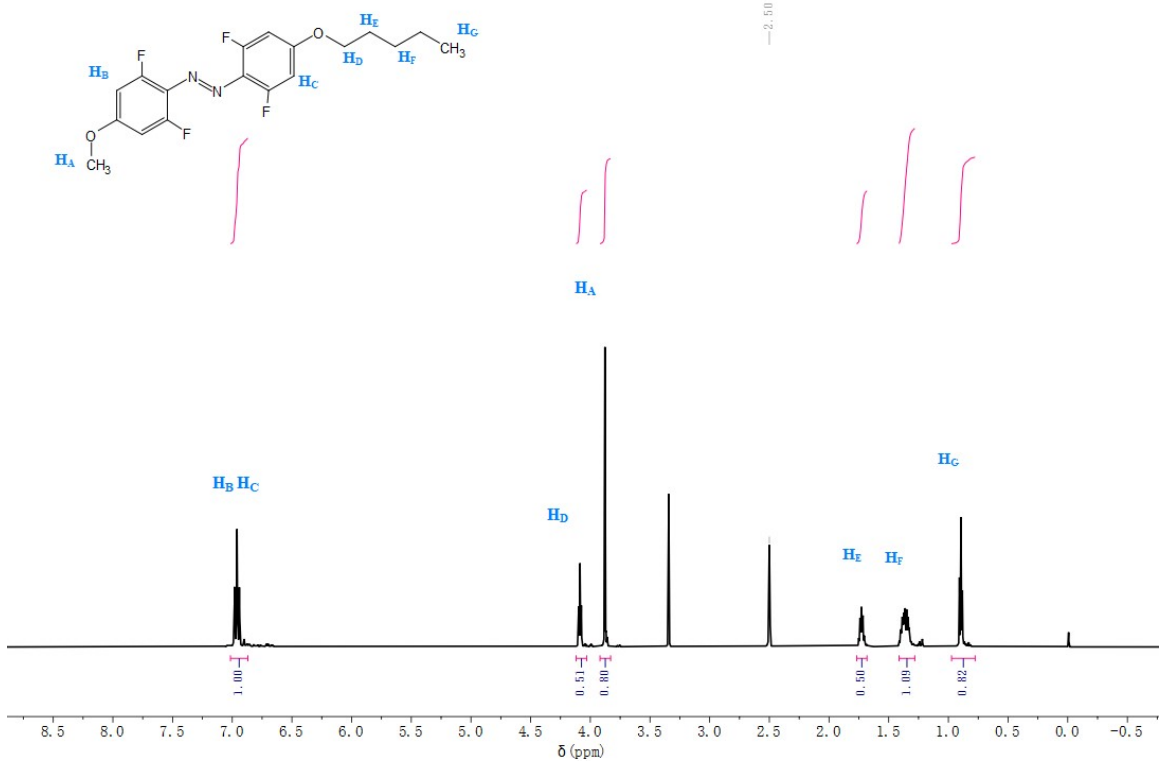
1. The structure of R6N.



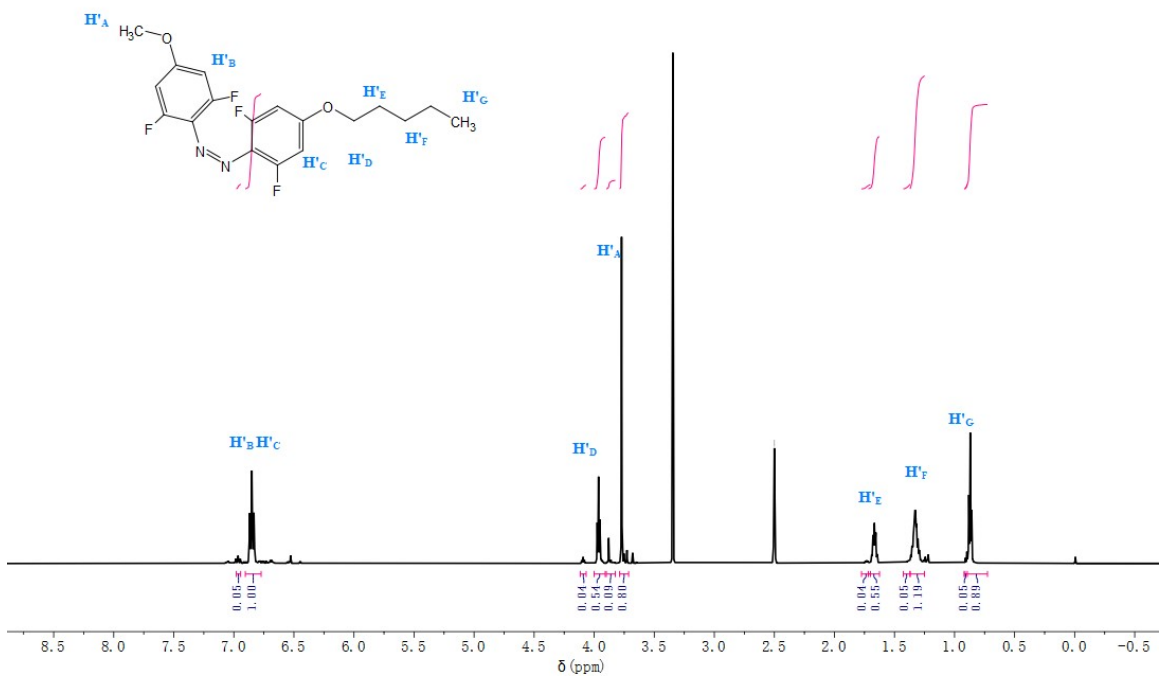
R6N

2. Structural spectra characteristic of azobenzene-based molecule (Azo-C5)

Azo-C5 (Initial)



Azo-C5 (PSS365)



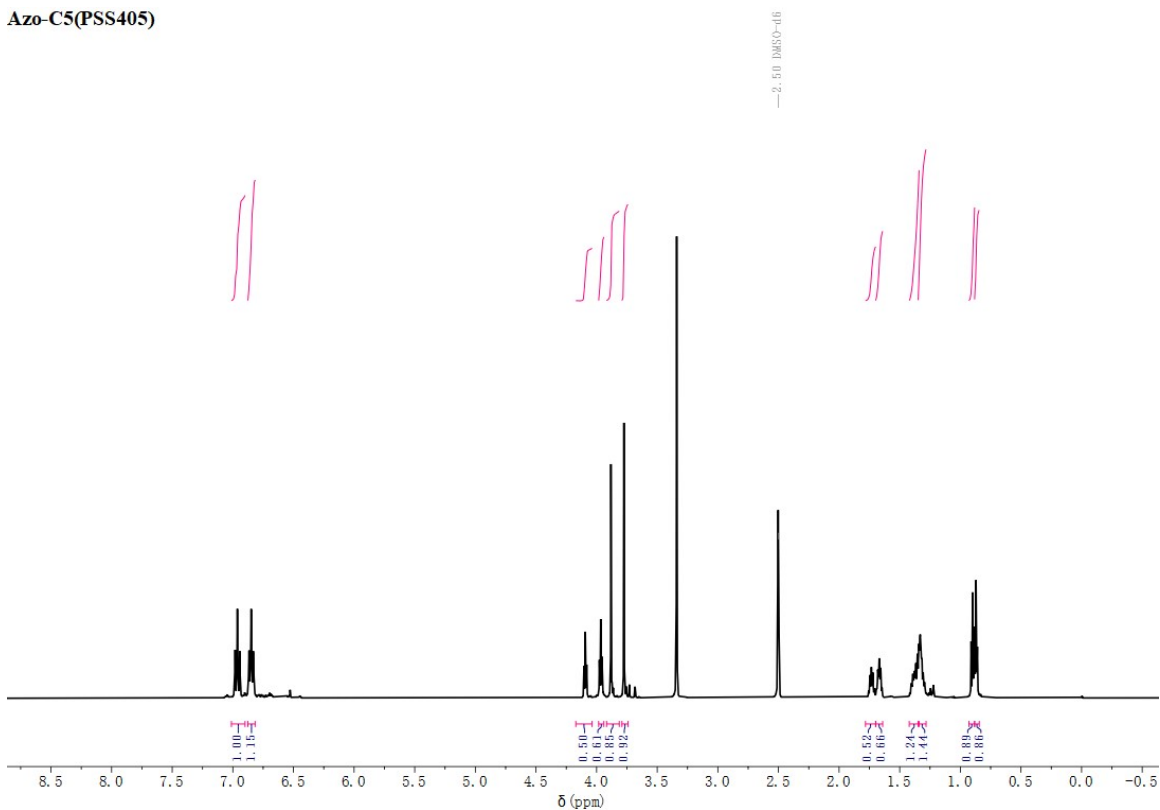


Fig. S2 ^1H NMR spectra of Azo-C5 in DMSO- d_6 at PSS $_{365}$ and PSS $_{405}$.

3. UV-vis absorption spectra of Azo-C5 under different wavelengths irradiations

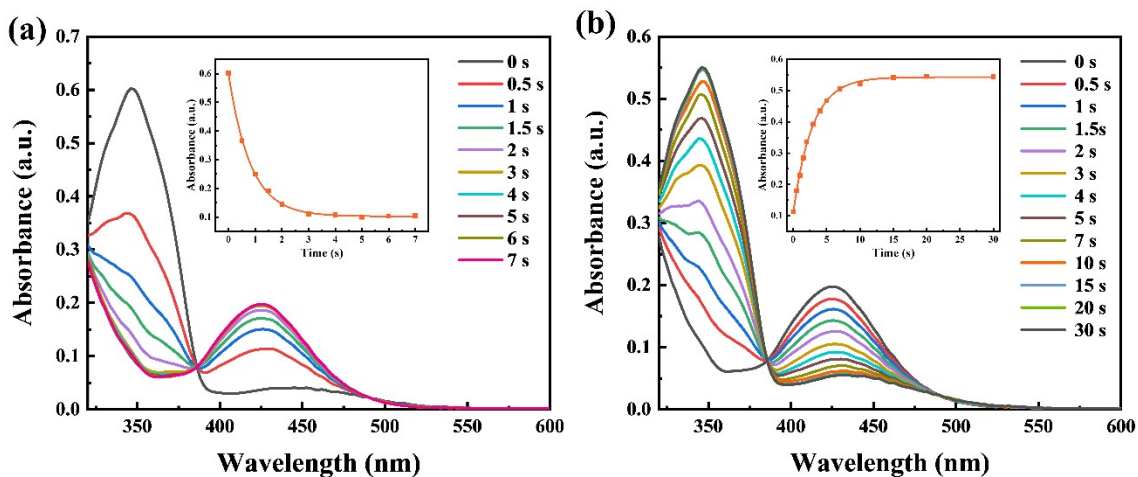


Fig. S3 (a-b) UV-visible absorption spectrum of Azo-C5 (0.0102 mol/L in HNG60800) at 365 nm (80 mW cm^{-2}) and 405nm (54 mW cm^{-2}). The illustration shows the absorption spectra of Azo-C5 at 350 nm.

The change of chemical structures of Azo-C5 under the photoisomerization process corresponds to the decrease of the absorption band at 350 nm ($\pi \rightarrow \pi^*$ transition) and a tiny increase in the band at 405 nm ($n \rightarrow \pi^*$ transition) during the 365 nm light irradiation process. Lights of 405 nm irradiated the sample, converting the cis state into a trans state.

4. The temperature response of the helical twisting power (HTP, β) of R6N in CLCs

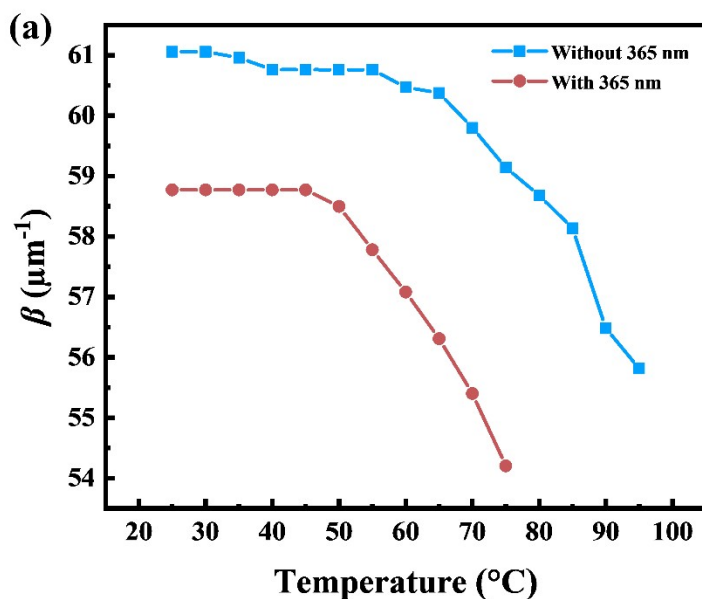


Fig. S4 variation of β with temperature for R6N in HNG60800 liquid crystals containing Azo-C5 before and after 365 nm illumination.

Furthermore, the R6N also exhibits temperature response, as shown in Fig. S4a. The β of the R6N was reduced upon heating. Under the UV light, the β of R6N was $58.8 \mu\text{m}^{-1}$ from 25 °C to 45 °C. Upon heating to 45 °C, β rapidly decreased to an undetectable value, arriving at the isotropic state at 76 °C.

5. Measurement of helical twisting power (β)

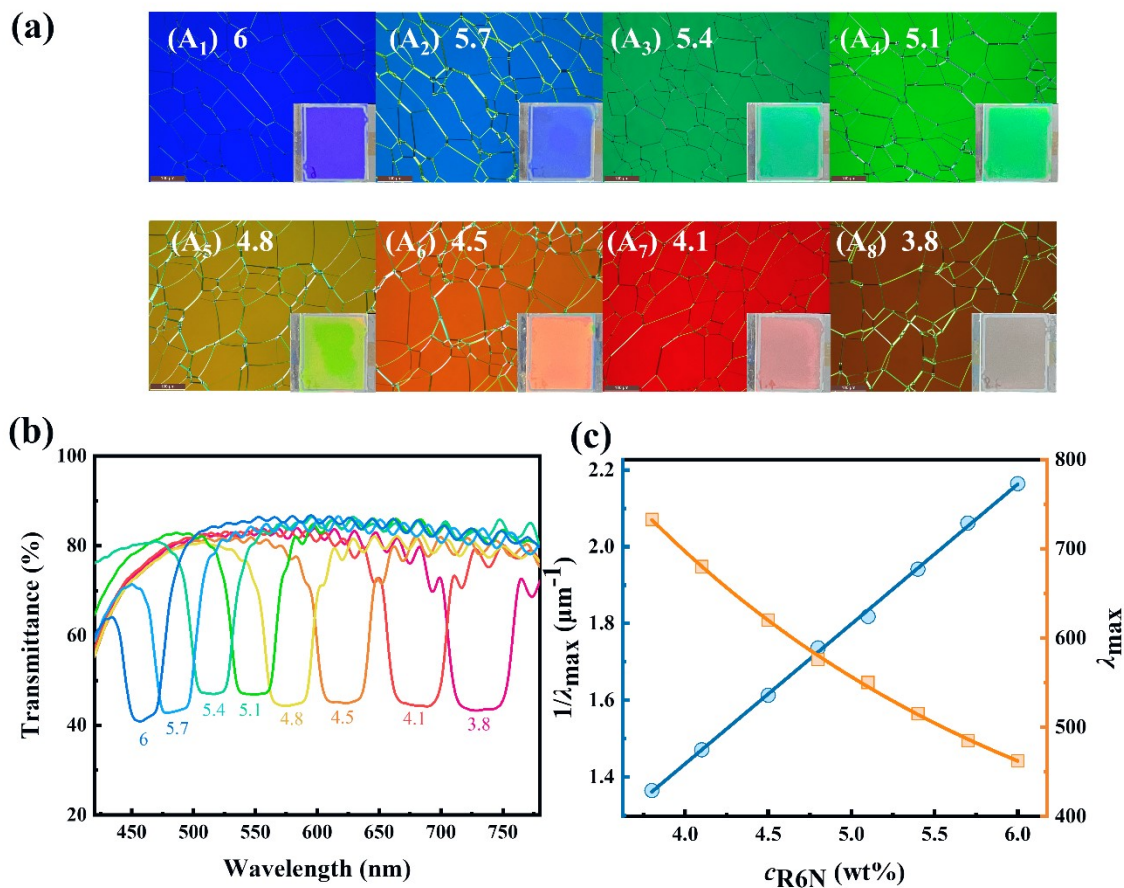


Fig. S5 (a) Concentration-dependent POM images and (b and c) transmittance spectrum changes of CLC mixtures composed of R6N and HNG60800 at 25°C. Insets are the photos of real LC cells. The composition ratio of R6N is (A₁) 6 wt%, (A₂) 5.7 wt%, (A₃) 5.4 wt%, (A₄) 5.1 wt%, (A₅) 4.8 wt%, (A₆) 4.5 wt%, and (A₇) 3.8 wt%.

The CLC samples were prepared by doping the chiral dopant R6N into the LC host HNG60800 and filled into 7 μm thick antiparallel aligned LC cells. The color of texture and λ_{max} at different concentrations were investigated using polarized optical microscopy and transmission spectrum, as summarized in Fig. S5a and S5b.

As the R6N concentration increased from 6 wt% to 3.8 wt%, the color of the planar texture in the samples shifted from blue-red to green-orange, yellow, and finally to red. The λ_{max} gradually experienced a redshift with the decreased concentration of R6N. The insets show

images of actual LC cells at each concentration. Correspondingly, the red shift of the λ_{\max} varied from 462 to 485, 515, 550, 576, 620, 680, and 733 nm.

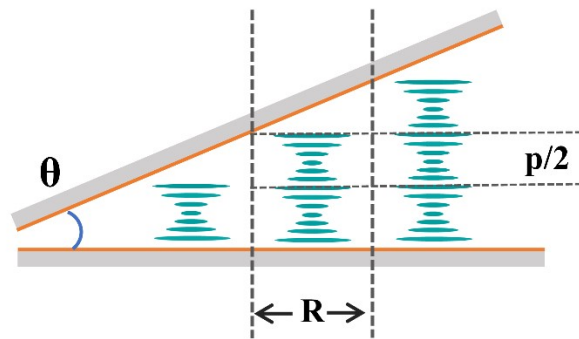
$$\lambda = np \quad (1)$$

$$\beta = \frac{1}{cp} \quad (2)$$

$$\frac{1}{\lambda} = \frac{\beta}{n} \quad (3)$$

In theory, we can derive equation (3) from Bragg's equation, which is equation (1) and equation (2). In the given equations, n is the average refractive index of the LC host, p is the pitch length of the helix, and c is the concentration of the chiral dopant. The blue circle and orange block are the experimental values of $1/\lambda_{\max}$ and λ_{\max} , respectively. Moreover, the blue and orange straight lines are the linear fit. As shown in Fig. S5c, $1/\lambda_{\max}$ is proportional to the concentration of R6N, indicating that our experiment agrees well with the theoretical calculations.

6. Determination of β before and after light exposure by the racemic method



Grandjean-Cano wedge method is a conventional technique for pitch measurement. A wedge cell with an opening angle is made by applying two different-sized spacers at each end of the cell. If the alignment of the substrates is planar (the director lies parallel to the

surface) and the rubbing directions of substrates are parallel to one another, the CLC becomes discrete. Because the value of the pitch and the alignment are fixed, the CLC arranges itself, as shown in sketch. This arrangement results in disclination lines between areas that contain a different number of layers. The difference in thickness between each domain must be $p/2$ to satisfy the alignment boundary condition.

The disclination lines of the CLC in the wedge cell can be seen through a polarized optical microscopy. The pitch was determined by the equation $p = 2R \tan \theta$, where R represents the distance between the disclination lines and θ is the wedge angle of wedge cells (EHC, KCRK-07, $\tan \theta = 0.0183$). The inverse of pitch proportionally increases with an increase in the concentration of a chiral dopant, according to equation (2). CLC is prepared by weighing appropriate amounts of the primary LC and dopant into a vial and mixing them with thorough stirring. The injection of the mixture into the wedge cell was carried out at room temperature.

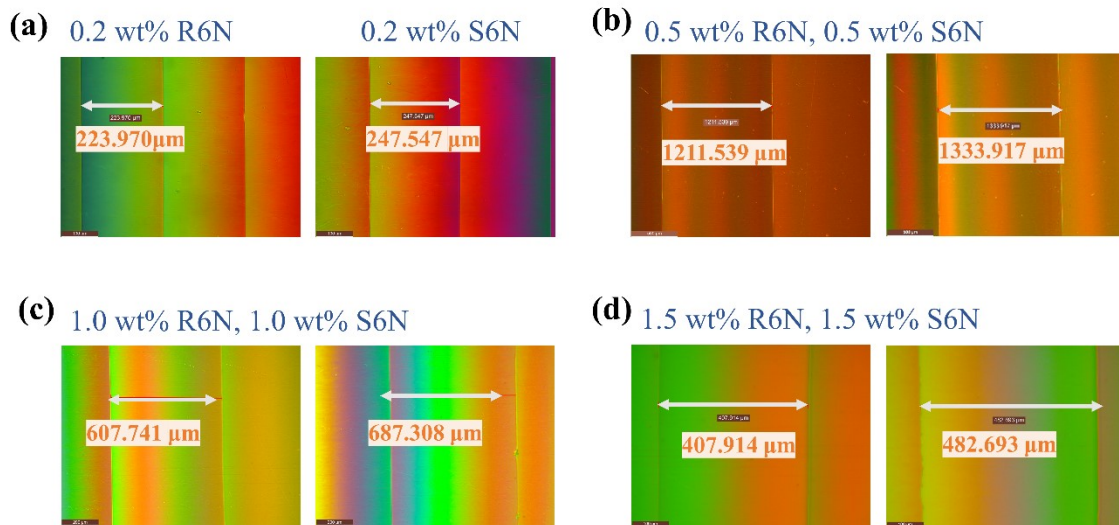


Fig. S6 The disclination lines measured by the deconvolution method are for a) 0.2 wt% R6N and 0.2 wt% S6N, b) 0.5 wt% R6N, and 0.5 wt% S6N, c) 1.0 wt% R6N, and 1.0 wt% S6N, d) 1.5 wt% R6N, and 1.5 wt% S6N in HNG60800.

Table S1 Helical twisting powers (β , mass ratio, μm^{-1}) of R6N in HNG60800 host as determined by Cano's Wedge method under irradiation by lights of different wavelengths.

The data is calculated from Fig. S6.

	0.1 wt% R6N		0.5 wt% R6N		1.0 wt% R6N		1.5 wt% R6N		2.5 wt% R6N	
			0.5 wt% S6N		1.0 wt% S6N		1.5 wt% S6N		2.5 wt% S6N	
	Initial	PSS ₃₆₅								
R (μm)	447.47	470.43	1211.54	1333.92	607.74	687.31	407.92	482.69	264.58	346.82
P (μm)	16.38	17.22	44.34	48.82	22.24	25.16	14.93	17.67	9.68	12.69
β (μm^{-1})	61.06	58.08	2.26	2.05	2.25	1.99	2.23	1.89	2.07	1.58